

Interaction between ferromagnetic resonance and spin currents in nanostructures

O. Rousseau and M. Viret

Service de Physique de l'Etat Condensé, CEA Saclay, DSM/IRAMIS/SPEC bat 772, CNRS URA 2464, F-91191 Gif-sur-Yvette, France

(Received 19 October 2011; revised manuscript received 13 January 2012; published 18 April 2012)

We report here on the detection of ferromagnetic resonance in a permalloy nanostructure using the inverse spin-Hall effect in a platinum layer in contact. The tiny spin currents driven out of the precessing magnetization of a micron square sized structure generate an electrical voltage in the platinum layer because of spin-orbit scattering. We have achieved isolating this signal from other resistive contributions and show that it dominates in certain field geometries. This detection technique can therefore be applied in ferromagnetic nanostructured materials under certain experimental precautions. We also have been able to modify the damping of our Py nanostructures by injecting spin polarized currents using the spin-Hall effect in Pt.

DOI: [10.1103/PhysRevB.85.144413](https://doi.org/10.1103/PhysRevB.85.144413)

PACS number(s): 73.63.-b, 85.75.-d

This last decade has seen an impressive surge of work on electronic transport and magnetization dynamics in mesoscopic systems containing nanomagnets, thus developing a new generation of spintronic devices.¹⁻³ Standard electronic devices use the conduction electrons' charge, whereas spintronics aims at using their spin. For this goal, the understanding of spin currents, their generation, and their interaction with magnetization or charge currents is required. Moreover, because of the constant drive for miniaturization, it is important to probe these effects in nanostructures.

One way to produce a spin current is to use the spin-Hall effect, a phenomenon based on the spin-orbit interaction of a charge current which generates a transverse spin current in a conductor.^{4,5} The interaction also produces the reverse effect called the inverse spin-Hall effect (ISHE), where a *pure* spin current in a nonmagnetic metal produces a transverse charge current. This has been used as a method for sensing spin currents, as the transverse charge current can generally produce a measurable voltage. It has also been predicted and measured that a ferromagnet driven to resonance by a radio-frequency field emits a spin current. This is due to the effect of damping which transfers some angular momentum to conduction electrons that can diffuse to a neighboring normal metal. This spin current converts into a charge current in metals with strong spin-orbit coupling like Pt. Recently, several papers have reported on the detection of this spin current in dynamical measurements,⁶⁻¹⁰ all in long bilayer stripes in order to amplify the detected voltage which scales with the ferromagnetic structure length. At the micron scale and below, only spin currents induced by DC charge currents have been detected by ISHE,¹¹ because these are generally two orders of magnitude larger than spin currents generated in dynamical experiments. It is therefore important to study how small a ferromagnet can be made before reaching the detection limit of its emitted spin current at resonance. This is the aim of the present study where we electrically detect the ferromagnetic resonance (FMR) of Ni₈₀Fe₂₀ (Py) nanostructures. The sample is composed of a circle and an ellipse made in Py and positioned on top of a 15-nm-thick Pt layer as shown in Fig. 1). It was fabricated using e-beam evaporation (for Pt) and sputtering deposition (for Py) with e-beam lithography, lift-off, and etching techniques. Part of the line is composed of a pure Pt stretch with no ferromagnetic material and is

used as a reference measurement. A broadband RF antenna is deposited close to the structure in order to transmit a microwave power, up to 40 GHz, reaching 9 dBm to the end of the stripline. The highest current density is reached in the terminating short thereby generating a microwave magnetic field $\mu_0 h_{rf}$ of the order of 1.5 mT in the center of the ellipse. In order to improve the signal detection, we use a square wave amplitude modulation of the RF power and measure with a lock-in detection the voltage generated at this frequency. All measurements were performed at 77 K.

When the applied frequency f and the static in-plane magnetic field \mathbf{H} fulfill the resonant conditions, the Py layer precesses and thus emits, by the spin pumping effect,^{12,13} a spin current perpendicular to the interface into the Pt layer (Fig. 2), which has both dc and ac components: $\vec{j}_s = (\hbar/4\pi)g^{\uparrow\downarrow}[\vec{m} \otimes \partial\vec{m}/\partial t]$, where \vec{m} is the unit vector of the magnetization \vec{M} and $g^{\uparrow\downarrow}$ the real part of the interface spin mixing conductance. As schematized in Fig. 2, this injected spin current is converted, by spin-orbit coupling, into a charge current by ISHE in the Pt layer:^{12,13}

$$\vec{j}_c^{\text{ISHE}} = \gamma_{\text{Hall}}(2e/\hbar)[\vec{n} \otimes \vec{j}_s]$$

where γ_{Hall} is the spin-Hall angle, and \vec{n} is the unit vector normal to the interface. This signal is detected as a voltage, V_{ISHE} proportional to \vec{j}_c^{ISHE} , that is maximum in a transverse geometry, i.e., for an in-plane magnetization perpendicular to the stripe direction (i.e., along y , see Fig. 2).

In our experiment, another signal is generated by rectification of the induction currents in the ferromagnet as first predicted by Juretschke¹⁴ and measured in various experiments.¹⁵⁻¹⁹ In our sample, the varying flux at the RF frequency induces a RF current I_{rf} that couples to any change of resistance at the same frequency to produce a dc voltage. The main resistance variation in our system originates from the component of anisotropic magnetoresistance (AMR) of the magnetic metal induced by precession. The AMR voltage reads

$$V_{\text{AMR}} = \Delta R_{\text{AMR}} I(t) \sin^2[\beta + \theta(t)]$$

where ΔR_{AMR} is the total variation of resistance due to AMR, β is the angle between the equilibrium magnetization and the current lines, and $\theta(t)$ is the small precession angle of the magnetization around its equilibrium. Because of our planar

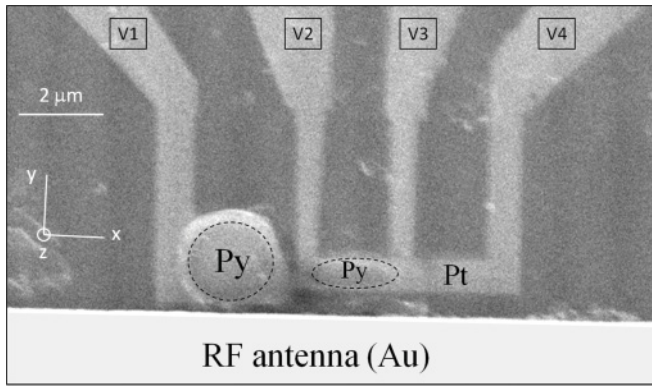


FIG. 1. SEM image of the device consisting of a 15-nm-thick Pt stripe including four contacts with two 20-nm-thick Py structures deposited on top. These are composed of a 2- μm -diameter circle and an ellipse with a 2- μm -long axis parallel to the stripe (x) and a 600-nm-short axis in the transverse (y) direction and separated by 800 nm. The short end of a coplanar strip waveguide is adjacent to the bilayers at respectively 1.1 μm and 1.4 μm from the ellipse and the circle centers. It is made in a Ti(5 nm)/Au(140 nm) bilayer by optical lithography, e-beam deposition, and lift-off techniques, in a shape optimized for our kapton substrate.

geometry, $\theta(t)$ is mainly in plane and also rather small: about 5° in our case. This rectified contribution to the FMR signal tends to dominate in small structures, as the Hall voltage decreases with the transverse length. In order to disentangle the two contributions, one can take advantage of their different symmetry with respect to the magnetization direction. The ISHE, with an angular dependence in $\gamma_{\text{Hall}} \sin(\beta) \sin^2(\theta)$, is odd in \vec{M} . Things are more complicated for the AMR signal which has the $\sin(\beta) \cos(\beta) \theta(t)$ symmetry. Here, one has to find out how the precession $\theta(t)$ changes when \vec{M} is reversed (i.e., β rotates by 180°). From the Landau-Lifshitz equation, one can see that what counts is the vector product $\vec{M} \otimes \vec{h}_{rf}$. For a RF field perpendicular to the plane of our structure (\vec{M} being in-plane), this rotates with \vec{M} and thus leaves $\theta(t)$ unchanged. The obtained AMR is then even in \vec{M} . Figure 3(a) shows the raw measurement of the FMR induced voltage where a clear asymmetry between positive and negative fields can be seen. Then, adding and subtracting the positive and negative field curves allows us to extract two, even and odd, contributions of similar amplitude [Fig. 3(b)].

It is tempting to attribute the odd part to the ISHE and the even one to the AMR, but this is unfortunately not so simple. Indeed, in our experiment a small in-plane component of the rf excitation field also exists. It is due to a small tilting

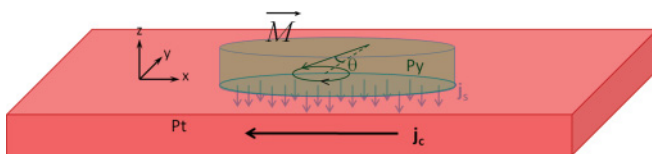


FIG. 2. (Color online) Schematics of the inverse spin-Hall effect signal. A spin current is generated in the nanostructure because of magnetization damping. It is converted into an electrical signal in the Pt by spin-orbit scattering and can be measured as a dc voltage peak at resonance.

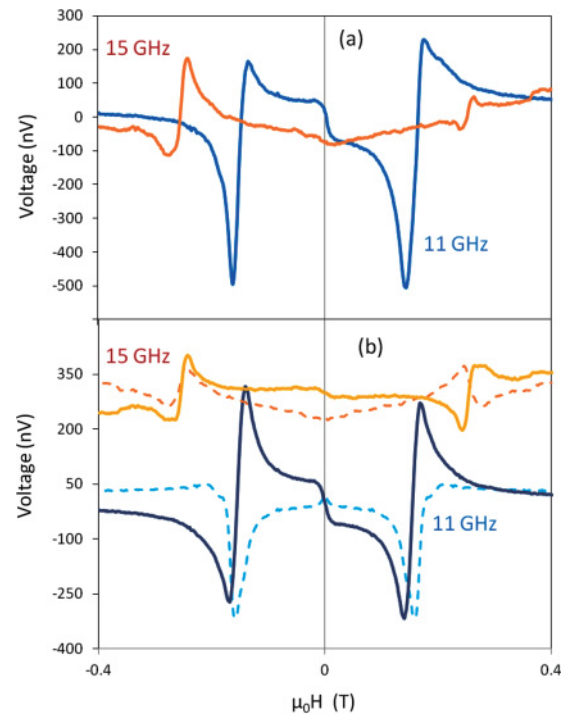


FIG. 3. (Color online) (a) Field dependence of the measured voltage for the ellipse ($V_3 - V_2$) at two different frequencies. The applied angle between H_0 and the current lines (i.e., the main direction of the ellipse or the x axis) is 60° , thus setting the magnetization at an angle close to 45° . (b) The odd (solid lines) and even (dashed lines) contributions are extracted by adding/subtracting the positive and negative field curves (11 GHz and 15 GHz curves are shifted for clarity).

of the excitation field angle along y , of the order of 3° , as the stripe is not exactly at the same height as the antenna (which is much thicker). Moreover, the RF field induced currents in the circuit also generate along y , at the level of the ferromagnetic nanostructures, a planar Oersted field. Its intensity can be estimated in the range of several Oersted, hence not negligible compared to the normal component of the RF field. When \vec{M} is reversed, this component changes its relative orientation in the referential given by magnetization and out-of-plane vectors, thus changing by π the angular phase of the precession angle induced by this field. This contributes to an odd voltage with the symmetry of $\sin(\beta) \cos^2(\beta) |\theta|$, which tends to dominate over the ISHE for arbitrary angles of \vec{M} , as shown in Fig. 3. However, for a purely transverse (along y) magnetization, the AMR voltage (especially its odd component) goes to zero and the only remaining (odd) contribution is the ISHE. This signal can then be extracted for transverse fields above the nanostructure saturation, as shown in Fig. 4. A residual AMR contribution, mainly even in field, is still visible, but the ISHE contribution dominates. The odd AMR residual contribution being in $\sin(\beta) \cos^2(\beta)$, it is of second order (estimated to be lower than 2 nV, hence in the measurement noise). An extra complication of the technique comes from the fact that, because our dc contacts are not adapted to microwave, the induced currents have a phase Φ that varies with frequency. Hence, the measured voltages can have Lorentzian or Lorentzian derivative shapes depending

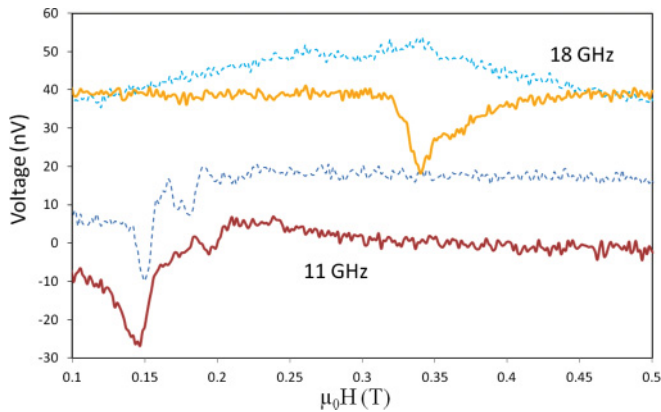


FIG. 4. (Color online) Transverse field dependence of the measured voltage for the ellipse at two frequencies: 11 GHz and 18 GHz. The solid and dashed curves correspond respectively to the odd and even contributions. All peaks on the odd parts are negative and have a similar shape. They are due to the ISHE, whereas the even contributions stem from a residual AMR effect (the AMR contribution to the odd part is estimated below the noise level).

on the frequency, which can complicate the analysis. Despite this, in the transverse geometry, an ISHE signal of about 20 nanovolts can be measured. The signal is found proportional to the RF power, and its value of 20 nV is in good agreement with the value of 40 nV calculated for a 5° precession angle using the formula given by Mosendz *et al.*¹⁰ (for the frequency of 18 GHz). The difference between measurement and calculation could originate from a different spin diffusion length in our Pt,²⁰ as well as the fact that the Py has an elongated but still ellipsoidal shape. It is to be noted that the precessing uniform mode should not occupy the full area of the nanostructure (it is more localized near the center) thus decreasing the relevant surface of spin current emission. This is taken into account in the estimate of the 5° precession angle, which is an average over the full nanostructure area. Importantly, unlike the AMR signal, the shape of the ISHE peak is independent of the frequency as the generated signal is directly a dc voltage (as in the normal Hall effect). The spin current density emitted in the platinum layer¹⁰ over the nanostructure area by the 5° amplitude of the precession is equivalent to that produced by a fully polarized charge current of $j_c \sim 5.10^4$ A/cm². It is also worth noticing that the same study on the circular nanostructure (measured in $V_2 - V_1$) gives results more difficult to analyze because the current lines are not as well defined as under the ellipse. Thus, although the resonance peaks are very clear, the extraction of the ISHE contribution from AMR contribution is much less accurate, the odd rectified AMR contribution is not reduced below the noise level and the shape of the odd signal always depends on the frequency.

In order to confirm the origin of our measured signal, we also performed measurements replacing Pt with Au. Pure Au is indeed known for its rather good spin transport properties, and it is therefore a poor spin to charge converter. As expected, the odd (ISHE) part of the measurement with a transverse magnetic field is, this time, much lower than the even part due to the AMR contribution as shown in Fig. 5. The peaks in the odd contributions are Lorentzian shaped and negative

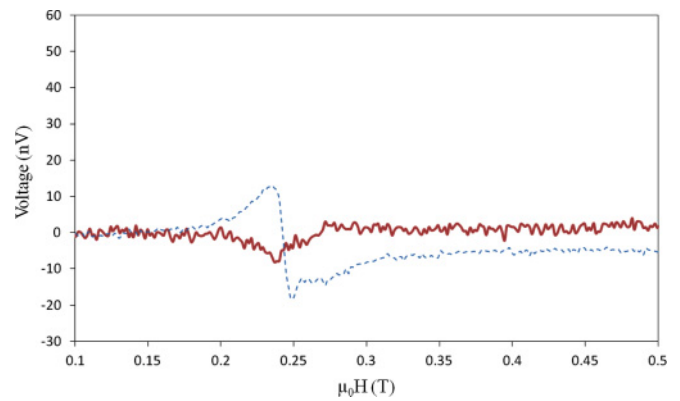


FIG. 5. (Color online) Transverse field dependence of the measured voltage for the ellipse in the Au/Py sample at a frequency of 15 GHz (on the same scale as that of Fig. 4). The solid curve is the odd contribution (from ISHE) and the dashed curve the even part (AMR contribution).

like those in the Pt sample, thus confirming their ISHE nature. They are about five times lower than the residual ones from the AMR contribution, consistent with the expected Hall angle ratio between Au and Pt given in Ref. 10.

It is also possible to study the reverse effect, i.e., the influence of an injected spin current on the ferromagnetic resonance shape of the nanostructures.^{20–22} Indeed, one can use the spin-Hall effect in Pt which spin polarizes the charge carriers in the perpendicular directions of a flowing dc current^{4,5} with the same symmetry as the Oersted field. In our geometry, a large current density in the Pt stripe can inject a spin current in the Py nanostructures in a direction that depends on the sign of the dc current. This spin current is supposed to have the effect of either enhancing or reducing the damping in the ferromagnetic layers, depending on the injected spins direction compared to the local magnetization.²² One of the difficulties of such a measurement is that the required current densities induce significant Joule heating susceptible to affect the damping by driving the sample's temperature close to the Curie point. Moreover, the Py structures are already in contact with Pt and their damping is thus deteriorated compared to a bare Py layer. To overcome these potential difficulties, it is convenient to subtract curves obtained at $+$ and $-I$, in order to pinpoint a possible difference with the current direction. Figure 6 shows that a strong current has indeed an effect on line shape with the right symmetry, where a negative/positive current amplifies/reduces the resonance amplitude. The features in these difference curves are found to appear for current densities above 3.10^6 A/cm², consistent with the report from Liu *et al.*²⁰ These are above the noise level, which demonstrates the effect of spin injection (due to the spin-Hall effect in Pt) on the damping in our Py structures. The data quality does not allow for a precise analysis of their shape, already intrinsically complicated by the nature of the signals (e.g., because of induced phases as discussed earlier). However, an amplitude analysis can already provide a reasonable estimate of the spin current effect on damping.⁸ We estimate here that a 6.10^6 A/cm² current density changes alpha by about 4%.

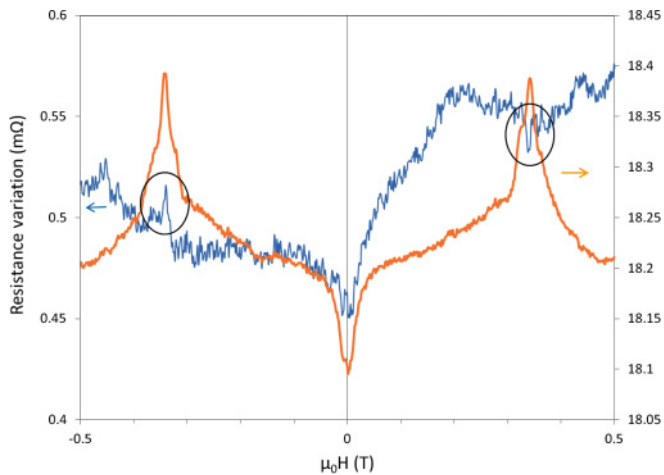


FIG. 6. (Color online) Effect of a dc current in the Pt stripe on the resonance shape of the elliptical Py nanostructure in a transverse field. The orange curve is the raw data measured when a positive current density of 6.10^6 A/cm² flows in the Pt layer, and the blue curve shows the subtraction of positive to negative current data. The amplification/reduction of resonance peak amplitude for negative/positive fields is consistent with a 4% change of the damping parameter due to spin injection.

In summary, we demonstrate here the detection of inverse spin-Hall effect on a single Py/Pt nanostructure induced by

uniform magnetization precession at resonance. At this small scale, the signal is mixed with other contributions generated by rectification effects of RF induction currents. The odd parity of the ISHE with the direction of magnetization is used to extract the relevant signal whose magnitude is consistent with reported Hall angle values. One way to optimize the detection of the dynamically generated spin currents would be to reduce the induction currents at the RF frequency, which are responsible for the AMR effects. This could be done by limiting the circuit surface (but the improvement would not be spectacular) and increasing its impedance. The latter can be achieved if the voltage electrodes could be made with tunnel junctions. In that case, induced currents could be significantly reduced, and the ISHE would be detectable from even smaller nanostructures. In view of the present signal amplitude, one could envision measuring spin currents from nanostructures ten times smaller in such a circuit. Finally, we have demonstrated that a strong current in the adjacent Pt layer can influence the resonance line shape of our Py structures. The symmetries with field and current direction as well as the order of magnitude of the effect are all consistent with a direct influence of spin currents generated in the Pt by spin-Hall effect.

We would like to acknowledge financial support from the French ANR contract “SUD” and the CNano “Balispin.” We also thank G. de Loubens for a critical reading of this manuscript.

- ¹A. Brataas, Y. Tserkovnyak, G. E. W. Bauer, and B. Halperin, *Phys. Rev. B* **66**, 060404 (2002).
- ²S. I. Kiselev, J. C. Sankey, I. N. Krivorotov, N. C. Emley, R. J. Schoelkopf, R. A. Buhrman, and D. C. Ralph, *Nature (London)* **425**, 380 (2003).
- ³S. Kaka and S. Russek, *Appl. Phys. Lett.* **80**, 2958 (2002).
- ⁴M. Dyakonov and V. Perel, *JETP Lett.* **13**, 467 (1971).
- ⁵J. Hirsch, *Phys. Rev. Lett.* **83**, 1834 (1999).
- ⁶K. Ando, J. Ieda, K. Sasage, S. Takahashi, S. Maekawa, and E. Saitoh, *Appl. Phys. Lett.* **94**, 262505 (2009).
- ⁷K. Ando, Y. Kajiwara, K. Sasage, K. Uchida, and E. Saitoh, *IEEE Trans. Magn.* **46**, 3694 (2010).
- ⁸K. Ando, Y. Kajiwara, S. Takahashi, S. Maekawa, K. Takemoto, M. Takatsu, and E. Saitoh, *Phys. Rev. B* **78**, 014413 (2008).
- ⁹O. Mosendz, J. E. Pearson, F. Y. Fradin, G. E. W. Bauer, S. D. Bader, and A. Hoffmann, *Phys. Rev. Lett.* **104**, 046601 (2010).
- ¹⁰O. Mosendz, V. Vlamincik, J. E. Pearson, F. Y. Fradin, G. E. W. Bauer, S. D. Bader, and A. Hoffmann, *Phys. Rev. B* **82**, 214403 (2010).
- ¹¹Y. Otani and T. Kimura, *IEEE Trans. Magn.* **44**, 1911 (2008).
- ¹²Y. Tserkovnyak, A. Brataas, and G. E. W. Bauer, *Phys. Rev. Lett.* **88**, 117601 (2002).
- ¹³Y. Tserkovnyak, A. Brataas, G. E. W. Bauer, and B. I. Halperin, *Rev. Mod. Phys.* **77**, 1375 (2005).
- ¹⁴H. Juretschke, *J. Appl. Phys.* **31**, 1401 (1960).
- ¹⁵M. V. Costache, S. M. Watts, M. Sladkov, C. H. van der Wal, and B. J. van Wees, *Appl. Phys. Lett.* **89**, 232115 (2006).
- ¹⁶M. V. Costache, M. Sladkov, S. Watts, C. H. van der Wal, and B. J. van Wees, *Phys. Rev. Lett.* **97**, 216603 (2006).
- ¹⁷M. V. Costache, S. M. Watts, C. H. van der Wal, and B. J. van Wees, *Phys. Rev. B* **78**, 064423 (2008).
- ¹⁸A. Yamaguchi, K. Motoi, A. Hirohata, and H. Miyajima, *Phys. Rev. B* **79**, 224409 (2009).
- ¹⁹A. Yamaguchi, K. Motoi, A. Hirohata, H. Miyajima, Y. Miyashita, and Y. Sanada, *Phys. Rev. B* **78**, 104401 (2008).
- ²⁰L. Liu, T. Moriyama, D. C. Ralph, and R. A. Buhrman, *Phys. Rev. Lett.* **106**, 036601 (2011).
- ²¹K. Ando, S. Takahashi, K. Harii, K. Sasage, J. Ieda, S. Maekawa, and E. Saitoh, *Phys. Rev. Lett.* **101**, 036601 (2008).
- ²²V. E. Demidov, S. Urazhdin, E. R. J. Edwards, M. D. Stiles, R. D. McMichael, and S. O. Demokritov, *Phys. Rev. Lett.* **107**, 107204 (2011).